Journal of Archaeological Science: Reports 60 (2024) 104813

Contents lists available at ScienceDirect

Journal of Archaeological Science: Reports

journal homepage: www.elsevier.com/locate/jasrep

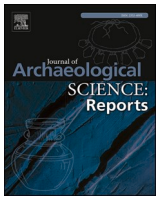

Petrological characterization for material provenance of *haniwa* earthenware from mounded tombs in the Kibi region, Japan

Toshio Nozaka [a,*], Naoya Ohbayashi [a], Yuki Toda [a], Kanako Sugiura [b], Takahiro Nozaki [c], Osamu Kimura [c], Naoko Matsumoto [c], Akira Seike [b]

[a] Department of Earth Sciences, Okayama University, 3-1-1 Tsushima-naka, Okayama 700-8530, Japan
[b] Department of Archaeology, Okayama University, 3-1-1 Tsushima-naka, Okayama 700-8530, Japan
[c] Research Institute for the Dynamics of Civilizations, Okayama University, 3-1-1 Tsushima-naka, Okayama 700-8530, Japan

ARTICLE INFO

Keywords:
Haniwa
Paste material
Provenance
Kofun
Kibi
Japan

ABSTRACT

To determine the provenance of the materials used in the production of *haniwa* earthenware unearthed from mounded tombs (*kofun*) in the Kibi region (modern Okayama Prefecture) during the Kofun period (late 3rd – 6th century CE) of Japan, we carried out petrological analyses of *haniwa* sherds, including optical microscopy, X-ray diffractometry, X-ray fluorescence spectroscopy, and electron-probe analysis. The 25 *haniwa* sherds analyzed from 12 representative mounded tombs are composed of mineral and rock inclusions with variable grain size set in a clay matrix. The dominant inclusions are quartz, K-feldspar, and plagioclase, associated with minor amounts of amphibole, volcanic glass, and granitic rocks in all the *haniwa* sherds, and small amounts of hornfels, quartz rock, and accessory minerals, including mica, ilmenite, and chromite, in some of the sherds. Amphibole and plagioclase have compositional variations indicative of the mixing of tephra and granitic components. The compositions of volcanic glass inclusions are similar to those of the Aira-Tanzawa and Kikai-Akahoya tephras widely distributed in southwestern Japan. Bulk chemical compositions show magmatic differentiation trends, which are variable between individual tombs. From these results, it is concluded that the paste materials of *haniwa* in the Kibi region were commonly derived from weathered granitic rocks mixed with minor amounts of three widespread tephras. The variations of chemical and mineralogical compositions are probably the reflection of local geologic settings, suggesting the presence of specific mining sites of paste materials around each tomb. The mining sites could be located at the bases of hills of granitic rocks covered by widespread tephras and in some cases, near the flood plain of big river systems.

1. Introduction

Ancient Japanese ceramics display variation in their physical characteristics, including shape, size, surface pattern, color, and hardness, which are variable between locations and periods, depending on the composition of raw materials, shaping techniques, and firing conditions. Quantitative analyses of these characteristics provide rigid bases for resolving archaeological questions, including the uniqueness of individual regions, interaction between regions, and the cultural and technological development of ancient society. In particular, petrological analyses are useful to infer the provenance of the paste materials of ceramics, because they are mainly made of rock-forming silicate minerals.

Haniwa are the unglazed earthenware that were arranged surrounding mounded tombs (*kofun*) during the Kofun period (late 3rd – 6th century CE) of Japan. They were modified from earthenware such as jars and ceremonial jar stands that had been used in the preceding Yayoi period (*ca.* 10th century BCE – early 3rd century CE) and can be found in a variety of shapes, including cylindrical, weapon-shaped, house-shaped, animal-shaped, or human-shaped. Among these, the cylindrical *haniwa* is the oldest type and its prototype most likely originated and developed to *haniwa* in the Kibi region (modern Okayama Prefecture) and subsequently spread to other regions of Japan (Kondo and Harunari, 1967). Therefore, investigation of cylindrical *haniwa* from the Kibi region and comparison with those from other regions can provide an important key to understanding interaction between regions and the cultural and technological development of ancient Japan; however, quantitative analyses using modern analytical techniques have been

* Corresponding author.
E-mail address: nozaka@cc.okayama-u.ac.jp (T. Nozaka).

https://doi.org/10.1016/j.jasrep.2024.104813
Received 31 May 2024; Received in revised form 22 August 2024; Accepted 10 October 2024
Available online 19 October 2024

insufficiently pursued.

Here we report the results of the petrological analyses of *haniwa* sherds unearthed from several representative mounded tombs in the Kibi region (Fig. 1). The Kibi region, which saw significant sociopolitical development during the Yayoi and Kofun periods, witnessed the construction of several large mounded tombs. These mounded tombs were constructed for various levels of the elite of society, from the huge Zozan *kofun* (350 m long) and Sakuzan *kofun* (280 m long), which are the fourth and tenth largest tombs in Japan, respectively, to the innumerable smaller tombs. *Haniwa* in the Kibi region typically have a cylindrical shape and their size changes throughout the Kofun period. The sherd samples analyzed in this study are fragments from cylindrical *haniwa* that would have originally measured around 40–60 cm tall and 20–30 cm in diameter, which is a size typical of examples produced in the Middle Kofun period (Fig. 2).

Microscopic observation and bulk chemical analysis with X-ray fluorescence spectrometry have independently been performed for *haniwa* from Zozan *kofun*, Sakuzan *kofun*, and a few other mounded tombs in the Kibi region, and showed the presence of three or four groups with distinctive mineralogical or chemical compositions, suggesting a difference in material provenance (e.g., Okuda, 1990; Harunari et al., 2016; Hirakawa et al., 2018). To demonstrate the material provenance in more detail, we carried out multi-technique, modern petrological analyses, i.e., microscopic observation, X-ray diffractometry, X-ray fluorescence spectrometry, and electron-probe analysis of *haniwa* from the Kibi region, including those from several other tombs than previously studied to see regional and temporal variations. From characterization based on texture, mineral abundance, bulk chemical composition, and chemical composition of individual mineral components, we obtained lines of evidence for the provenance of the paste materials of *haniwa*, which could be a key to understanding the characteristics of the culture of the Kibi region in ancient Japan. Our results show the advantage of multi-technique analyses for better understanding of provenance of *haniwa* and ancient ceramics.

2. Description of materials

Twenty-five sherds of cylindrical *haniwa* unearthed from 12 mounded tombs (Fig. 1) were analyzed in this study (Fig. 2): Three from Zozan (sample# ZZ1-3), three from Sakuzan (SZ1-3), four from Tenguyama (TG1-4), six from Nima-otsuka (NO1-6), two from Moriyama (MO1-2), and one from each of Shuku-terayama (ST), Horen-22 (HR), Oshikiyama (OS), Kotsukuriyama (KT), Kotsukuriyama-nishi-3 (KTN), Iwata-3 (IW), and Miyayama-4 (MI). The location of these tombs and their construction periods, inferred from the shape and surface pattern of their *haniwa* (Nozaki, 2017; Kimura, 2023) are shown in Fig. 1 and Table 1, respectively. Four tombs (Horen-22, Oshikiyama, Kotsukuriyama, and Kotsukuriyama-nishi-3) built in the Misu Hills and three tombs (Iwata-3, Miyayama-4, and Moriyama) in Akaiwa City are included together for convenience of description. Although the number of samples from each mounded tomb was limited due to considerations of cultural property protection, we attempted to analyze samples from as many tombs across the Kibi region as possible in order to see regional and chronological variations.

Most of the *haniwa* sherds are brown or reddish brown in color on both their surface and cross-section, while some are grey, dark grey, or blackish (Fig. 2). In general, greyish earthenware (known as “Sue type”) is harder and more compact than brownish examples (“Haji type”), suggesting that the former type was fired in tunnel kilns, which were introduced to Japan in the Kofun period, at higher temperatures and greater reducing conditions than the latter type, which were open-fired using traditional methods. Four samples of *haniwa* sherds (SZ3, NO4, MO1, and MO2) are Sue type and the others are Haji type (Fig. 2).

Four samples of rocks (a two-mica granite, a two-mica granitic aplite, a psammitic hornfels, and a pelitic hornfels) were collected from outcrops near the Nima-otsuka and Tenguyama tombs and analyzed in this study for comparison of muscovite compositions.

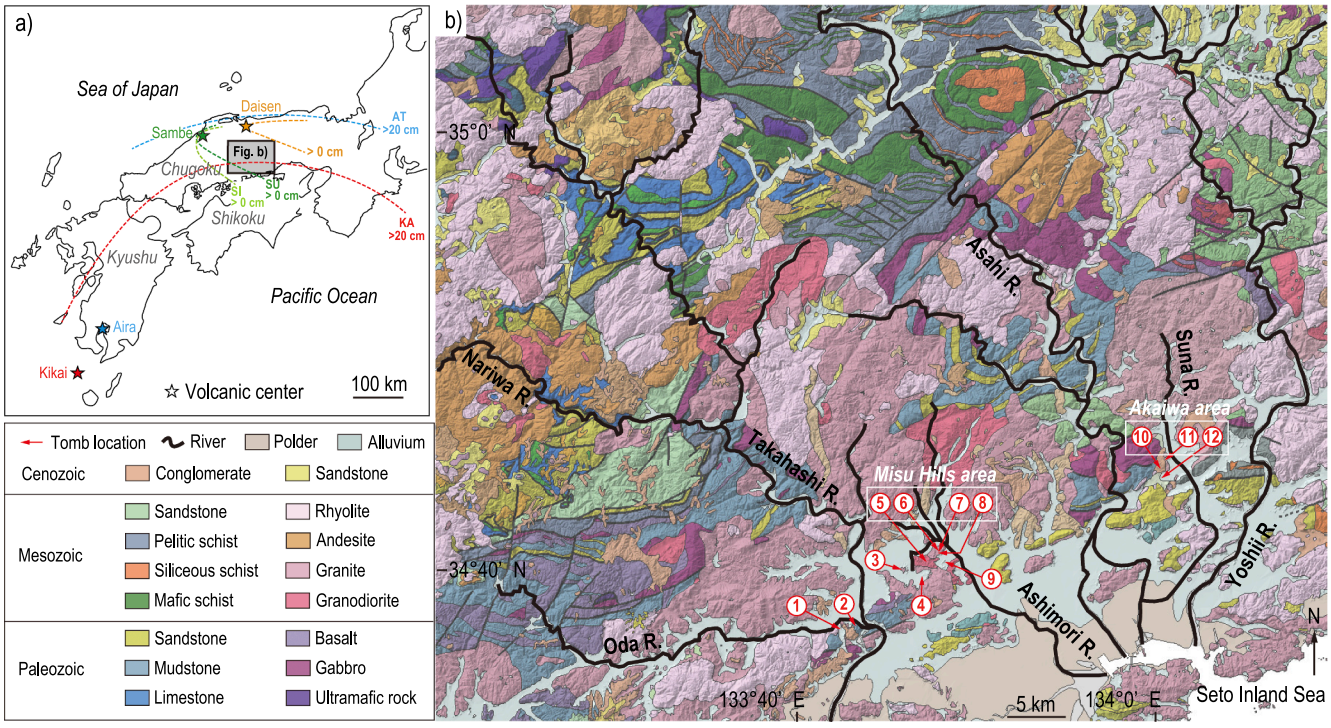

Fig. 1. (a) Map showing the distribution, thickness, and volcanic center of eruption of the Aira-Tanzawa (AT), Kikai-Akahoya (KA), Sanbe-Ukinuno (SU), Sambe-Ikeda (SI), and Daisen tephras (Machida and Arai, 2003). (b) Geological map of the Kibi region (Geological Survey of Japan, 2022), showing the locations of mounded tombs from which studied haniwa sherds were unearthed: 1. Nima-otsuka; 2. Tenguyama; 3. Sakuzan; 4. Shuku-terayama; 5. Horen-22; 6. Oshikiyama; 7. Kotsukuriyama; 8. Kotsukuriyama-nishi-3; 9. Zozan; 10. Iwata-3; 11. Miyayama-4; and 12. Moriyama.

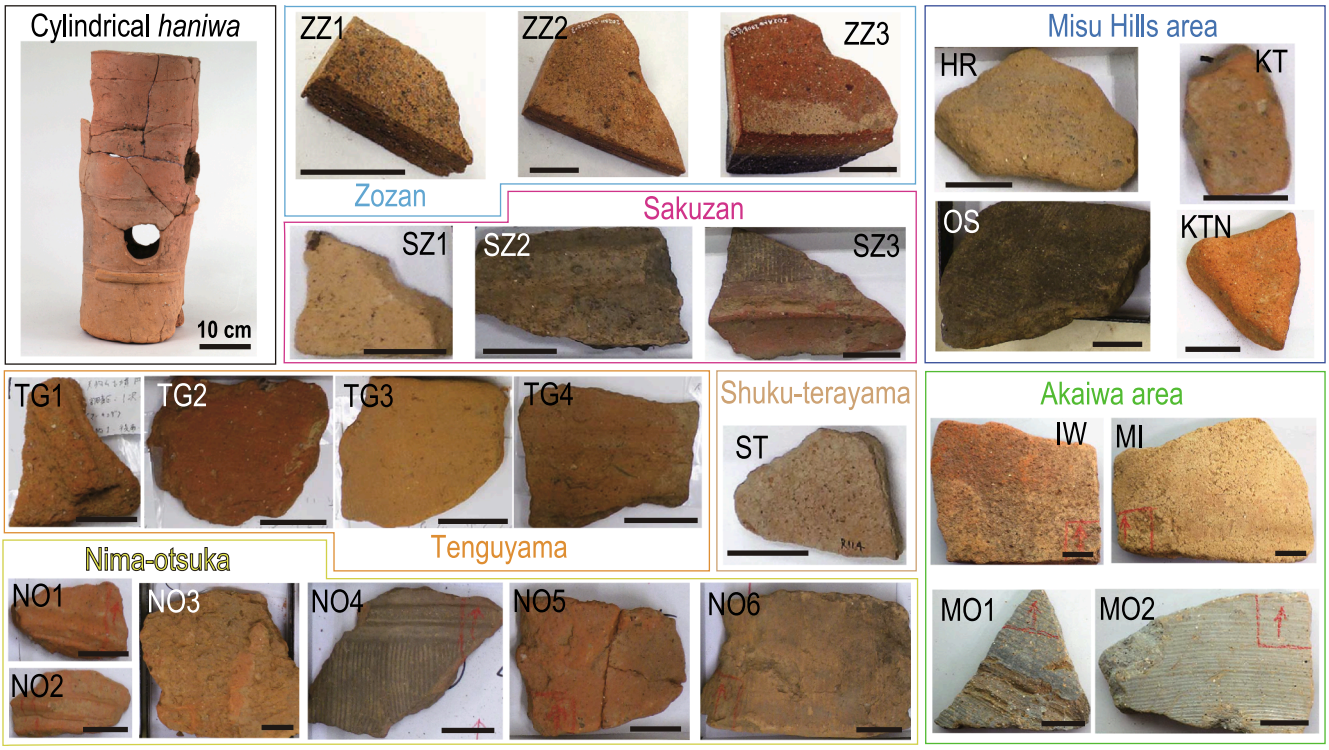

Fig. 2. Photographs of a representative cylindrical *haniwa* reconstructed by assembling sherds unearthed from Tenguyama *kofun* (upper left) and the *haniwa* sherd samples analyzed in this study. Scale bars for the samples (bottom of pictures) indicate 2 cm.

Table 1
Construction period of the mounded tombs from which studied *haniwa* sherds were unearthed.

	5th century			6th century
	early	middle	late	middle
	Zozan (ZZ)	Sakuzan (SZ)	Tenguyama (TG)	Nima-otsuka (NO)
			Shuku-terayama (ST)	
Misu Hills area	Oshikiyama (OS)		Horen-22 (HR)	
		Kotsukuriyama (KT)	Kotsukuriyama-nishi-3 (KTN)	
Akaiwa area	Iwata-3 (IW)	Miyayama-4 (MI)	Moriyama (MO)	

Construction periods were inferred from the archeological characteristics of the *haniwa*, including shape and surface pattern (Nozaki, 2017; Kimura, 2023). Abbreviations in parentheses are used for sample numbers.

3. Analytical methods

Chips of 4–6 cc volume were cut from the *haniwa* sherds using diamond disks without water or lubricant liquid. Polished thin sections were prepared from parts of the chips for optical microscopy, observation of back-scattered electron image (BEI), and analysis using electron-probe microanalyzer (EPMA). The rest of the chips were ground to make powder samples for analyses using X-ray diffractometer (XRD) and wavelength dispersive X-ray fluorescence spectrometer (XRF).

Mineral identification and textural observations were carried out using an ordinary petrographic microscope with plane-polarized lights (PPL) and crossed polarizers (XPL). Fine-grained opaque minerals were identified by semi-quantitative chemical analysis using an energy-dispersive X-ray spectrometer set on an EPMA.

Semi-quantitative bulk mineral compositions were determined through XRD using a Malvern PANalytical Aeris at Okayama University, with Cu-Kα radiation at 40 kV and 15 mA, and a scanning range of 2θ from 5° to 90° with a rate of 0.27°/s. Obtained diffraction data were processed using the software QualX ver. 2.24 with the COD database for assignment of diffraction peaks to rock-forming minerals.

Bulk chemical compositions were analyzed through XRF using a Rigaku ZSX Primus II at Okayama University, with glass disks made from 1.8 g ignited sample powder fused with 3.6 g $LiBO_2$-$Li_2B_4O_7$ (80:20) flux. Concentrations of 10 elements (Si, Ti, Al, Fe, Mn, Mg, Ca, Na, K, and P) were obtained using rock standard samples (JA-1, JA-2, JA-3, JB-1a, JB-2, JB-3, JG-1a, JG-2, JG-3, JR-1, JR-2, JGb-1 and JP-1) supplied by the Geological Survey of Japan.

Chemical compositions of minerals were analyzed through EPMA using a JEOL JXA-8230 at Okayama University with an accelerating voltage of 15 kV, a beam current of 20nA, and a probe diameter of 1–2 μm for silicates/oxides. After searching for optimal analytical conditions with no attenuation of X-ray intensity, a beam current of 7 nA and a probe diameter of 5–10 μm were adopted for volcanic glass. Counting time was 10 s at the peaks of characteristic X-rays and 5 s at background positions. Standards used were natural or synthetic oxides and silicates. The applied matrix corrections followed the procedures of Bence and Albee (1968) for silicates/oxides, using alpha factors of Nakamura and Kushiro (1970) and the ZAF correction for volcanic glass. The total amounts of oxides of analyzed volcanic glass were normalized to be 100 % on a volatiles-free base, though the amount of volatiles was estimated to be small (commonly less than the detection limit or up to 1 wt% at the maximum) in comparison with similarly normalized data reported in the literature.

4. Results

4.1. Petrographical and mineralogical analysis

All the analyzed *haniwa* sherds are similar in texture, and their mineral and rock inclusions, with angular to rounded shape and variable

size (<0.01 mm to 1 mm, with a few grains up to 2–4 mm in some sherds), are set in a very fine-grained clay matrix (Fig. 3a-h). No clear gap in grain size distribution of inclusions in each sherd is visible. The mineral inclusions mainly consist of quartz, K-feldspar, and plagioclase, with subordinate amounts of amphibole (hornblende in the broad sense; i.e., calcic amphibole with a brownish or greenish color) and volcanic glass, and trace amounts of biotite, muscovite, cummingtonite, orthopyroxene, zircon, epidote, rutile, and/or opaque minerals including magnetite, ilmenite, and chromite. Relatively coarse grains (> 0.1 mm) are frequent in the cases of quartz, K-feldspar, plagioclase, and rock inclusions, and rare in the other minerals.

The basic features of each mineral inclusion observed under the petrographic microscope are as follows. Quartz occurs as clear crystals with no effect of alteration. K-feldspar typically exhibits a perthite structure with Na-feldspar exsolution. Plagioclase frequently shows a zonal structure. Amphibole (hornblende) grains have prismatic shape and greenish or brownish pleochroism, and particularly in Sue-type *haniwa*, they are altered to opaque pseudomorphs including tiny magnetite grains. Biotite grains in most of the analyzed sherds are altered to brown-colored, lower birefringent pseudomorphs. Volcanic glass has a shape of bubble-wall type in most cases and of pumice type in some cases (for shape classification of volcanic glass, see Heiken, 1972; Machida and Arai, 2003).

All the sherds contain a small amount of fine-grained (< 1 mm, by definition in igneous petrology) granite or granodiorite fragments, and some sherds also contain fine-grained granophyre and/or aplite (much finer-grained than the granite) fragments. These granitoid fragments are composed of more than one of quartz, K-feldspar, and plagioclase with or without amphibole, biotite, and muscovite; granitoid containing amphibole is referred to as granodiorite in this study. Quartz rock (quartzite or quartz vein), which commonly occurs in Nima-otsuka and Tenguyama *haniwa*, is an equigranular aggregate of tiny grains (0.02–0.1 mm) of quartz (Fig. 3e-h). Hornfels composed mainly of very fine-grained (typically < 0.03 mm) quartz, biotite, and muscovite occurs in some of the Nima-otsuka, Tenguyama and Sakuzan *haniwa* sherds. In addition, most of *haniwa* sherds have variable amounts of clay pellet, which is dark brown-colored, spherical material containing quartz and feldspar grains and typically surrounded by a ring-shaped void (Fig. 3e). The degree of optical activity of the clay matrix is moderate to high in most *haniwa* sherds, and low in some, particularly Sue-type sherds. Approximately 5–10 vol% of each sherd is occupied by parallelly arranged, elongated, or vugh-type voids (for matrix optical activity and void types, see Quinn, 2013).

The XRD analyses show that quartz, K-feldspar, and plagioclase are the most abundant minerals in all the sherds (Fig. 4), which is in agreement with the microscopic observations. Amphibole and biotite were not detected in the sherds that show the complete decomposition of these minerals under the microscope. Mullite and/or spinel were detected by XRD in Sue-type sherds (MO1, MO2, NO4, and SZ3) and some Haji-type sherds (KT and KTN).

Inclusions detected by microscopic observations and XRD analyses are summarized in Table 2. The inclusions of quartz, K-feldspar, and plagioclase in the *haniwa* sherds are similar in modal proportion and grain size to these minerals in granitic rocks widely exposed in the region around the mounded tombs (Fig. 1). Fine-grained granitic rocks included in the *haniwa* sherds commonly occur in granitic bodies in this region as well. Hornfels, which is included in the *haniwa* sherds from Nima-otsuka, Tenguyama, and Sakuzan, is exposed in the proximity of these mounded tombs, occupying a part of "mudstone" in the geological map (Fig, 1). Polycrystalline quartz inclusions in *haniwa* sherds are designated as 'quartzite' for simplicity but most of them are similar in texture to quartz veins intruded into hornfels in this region.

4.2. Bulk chemical composition

The bulk compositions of most of the *haniwa* sherds have SiO_2 contents (64–77 wt%; Fig. 5) comparable to typical granodiorite to granite, or dacite to rhyolite (Cox et al., 1979; Le Bas et al., 1986; Wilson, 1989), and granitoids (granites or granodiorites) from the Okayama and Kagawa areas in the Sanyo belt, southwestern Japan (Ishihara, 2003). This is consistent with the microscopic observations and XRD analyses indicating the dominance of granitic components. However, the *haniwa* sherds are enriched in FeO* (total iron as FeO) and Al_2O_3, and depleted in CaO and $Na_2O + K_2O$ (Fig. 5a-e). Most of the *haniwa* sherds show a tendency of decreasing Al_2O_3, FeO*, MgO, and CaO (Fig. 5a-d), and increasing FeO*/MgO and Na_2O/CaO ratios with increasing SiO_2 content (Fig. 5f, g). *Haniwa* sherds from the same mounded tombs tend to have similar compositions, with the exception of certain samples with distinctively higher/lower contents of SiO_2 and other oxides (e.g., SZ2 and NO1; Fig. 5). The XRF bulk chemical compositions are shown in the Supplementary data set.

4.3. Chemical composition of minerals

Chemical compositions of minerals are variable, reflecting the variation of their modes of occurrence, in particular, amphibole (Fig. 6a-c and 6h), feldspar (Fig. 6d-f and 6i), and volcanic glass (Fig. 6g-i). The chemical compositions of minerals are shown in the Supplementary data set.

4.3.1. Amphibole

Calcic amphibole shows a bimodal distribution of Mg/(Mg + Fe) mol ratio with one group of ~ 0.48–0.58 and the other of ~ 0.62–0.78 (Fig. 7a). The latter group occurs in almost all the *haniwa* sherds, whereas the former is restricted to *haniwa* from Zozan, Iwata-3, and the mounded tombs of the Misu Hills. The two types of amphibole can occur in the same sample, showing a contrast of brightness in BEI (Fig. 6a), where the brighter and darker areas are relatively Fe-rich and Mg-rich, respectively. The Fe-rich group is similar in composition to amphibole in granodiorite fragments (Fig. 6b), whereas the Mg-rich group is similar to amphibole associated with volcanic glass (Fig. 6h). In addition, Al and Ti contents of the two groups of amphibole respectively show similarities to amphibole in granodiorites from outcrops of the Ukan area, ~25 km northwest of the Misu Hills (Takagi, 1992), and to amphibole in tephras from the Sambe volcano (Fig. 7b and 7c; Hattori et al., 1983). These two groups of amphibole also show different arrays in the alkali-Si diagram (Fig. 7d), except for reaction rims of some grains, which contain tiny opaque grains (possibly magnetite) and have low alkali content (Fig. 6c and 7d).

Cummingtonite, which occurs rarely in some *haniwa* sherds (Table 2), has a composition of Fe-Mg amphibole with a deficiency of Ca (not shown in figures).

4.3.2. Feldspar

Feldspar is divided into two subgroups of solid solution; i.e., alkali feldspar with the endmember components of Or (K-feldspar) and Ab (Na-feldspar), and plagioclase with the endmember components of An (Ca-feldspar) and Ab (Na-feldspar). Alkali feldspar shows a compositional gap between Na- and K-feldspar (Fig. 8). One of the causes for this gap is the exsolution of albite in host K-feldspar (Fig. 6d), which typically occurs in granitic rocks. Plagioclase has compositions of labradorite, andesine, oligoclase, and albite, showing Ca/(Ca + Na) ratio variable in each mounded tomb (Fig. 8), in each *haniwa* sherd, and even in each grain, particularly in which compositional zoning is conspicuous (Fig. 6e). The fragmentation of a compositionally zoned grain as shown in Fig. 6e is one of the characteristics of plagioclase in volcaniclastics including tephra. Plagioclase associated with volcanic glass in a Nima-otsuka *haniwa* sherd shows an oscillatory pattern of compositional zoning (Fig. 6i) like the fragmented grain in Fig. 6e, and has higher Ca/(Ca + Na) than plagioclase in granitic rock fragments (Fig. 8). The wide range of Ca/(Ca + Na) variation, therefore, results from the mixing of plagioclase originating from granitoid and from tephra.

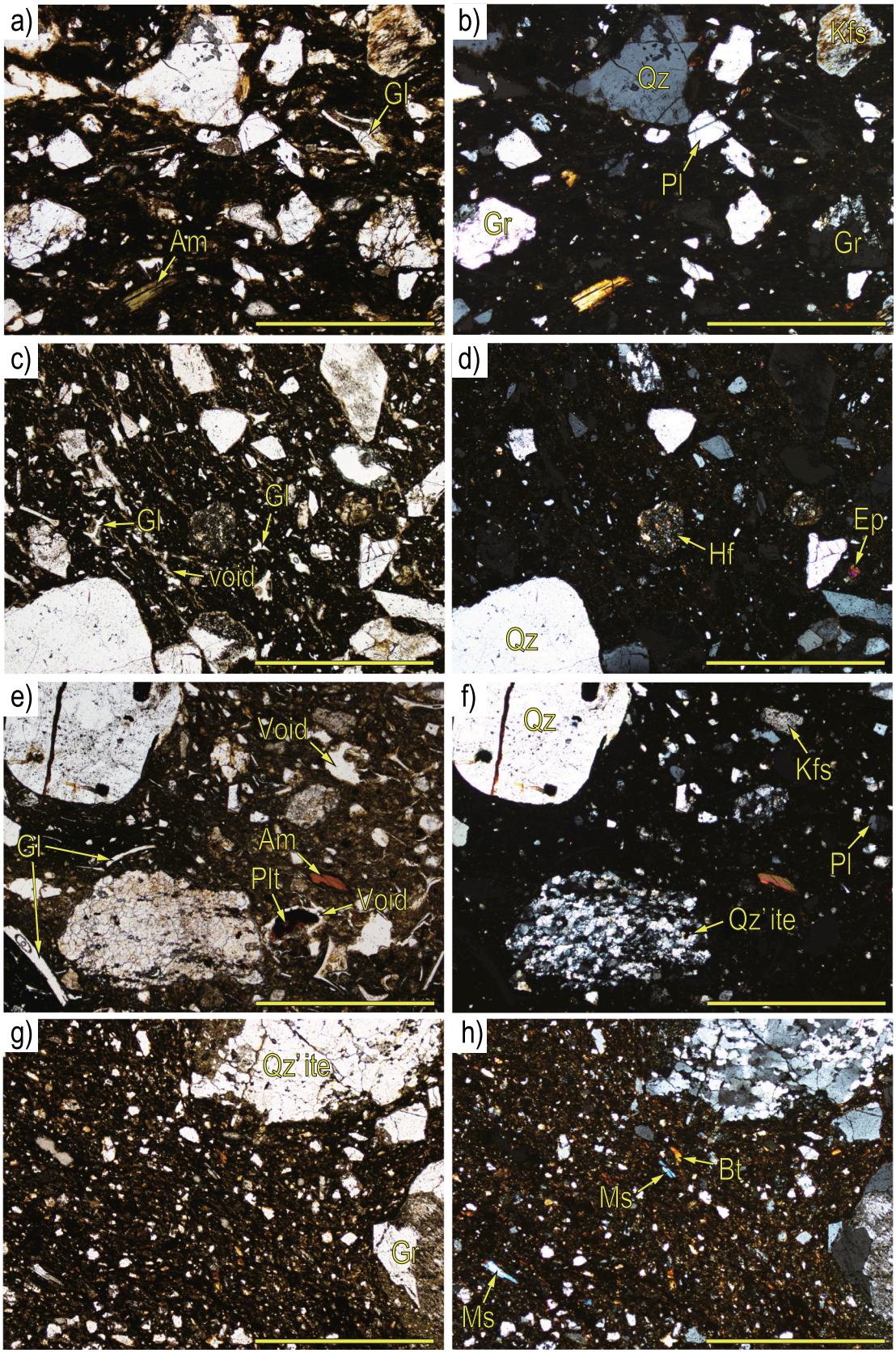

Fig. 3. Photomicrographs of representative *haniwa* sherd thin sections: (a, b) Zozan (ZZ2, PPL, and XPL); (c, d) Sakuzan (SZ2, PPL, and XPL); (e, f) Nima-otsuka (NO6, PPL, and XPL); (g, h) Tenguyama (TG4, PPL, and XPL). Abbreviations for minerals and rocks: Am, amphibole; Bt, biotite; Ep, epidote; Gl, volcanic glass; Gr, granite/granodiorite; Hf, hornfels; Kfs, K-feldspar; Ms, muscovite; Pl, plagioclase; Plt, clay pellet; Qz, quartz; Qz'ite, quartzite/quartz vein. Scale bars indicate 1 mm.

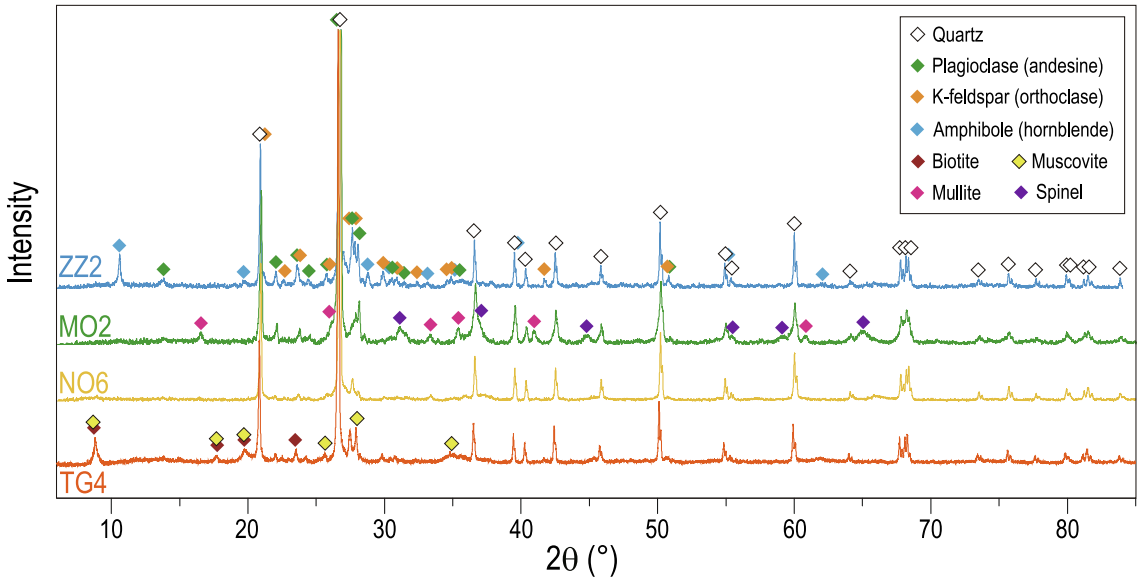

Fig. 4. Representative X-ray diffraction patterns of *haniwa* sherd samples. Diamond symbols with different colors indicate peak positions of minerals listed in the COD database.

Table 2
Minerals and rocks detected by microscopic observation and XRD analysis.

Mounded tomb	Sample#	Type	Qz	Kfs	Pl	Am	Bt	Gl	Other accessory minerals	Rock fragments
Zozan	ZZ1	Haji	xxx	xx	xx	x	x	x	Cum	Gr
Zozan	ZZ2	Haji	xxx	xx	xx	x	x	x	Cum, Apt, Ilm	Gr, Qz'ite
Zozan	ZZ3	Haji	xxx	xx	xx	x	–	x	Ms, Ep	Gr
Sakuzan	SZ1	Haji	xxx	xx	xx	x	–	x	Ilm	Gr
Sakuzan	SZ2	Haji	xxx	xx	xx	x	x	xx	Ms, Ep, Zr	Gr, Qz'ite, Hf
Sakuzan	SZ3	Sue	xxx	xx	xx	x	–	x	Mul, Ilm	Gr, Qz'ite, Hf
Shuku-terayama	ST	Haji	xxx	xx	xx	x	x	xx	Ms, Zr, Ilm	Gr
Tenguyama	TG1	Haji	xxx	xx	xx	x	x	x	Ms, Ep, Zr, Ilm	Gr, Qz'ite, Hf
Tenguyama	TG2	Haji	xxx	xx	xx	x	x	x	Ms, Ilm	Gr, Qz'ite, Hf
Tenguyama	TG3	Haji	xxx	xx	xx	x	x	x	Ms, Zr, Ilm	Gr, Qz'ite
Tenguyama	TG4	Haji	xxx	xx	xx	x	x	x	Ms, Ep, Ilm	Gr, Qz'ite, Hf
Nima-otsuka	NO1	Haji	xxx	xx	xx	x	x	xx	Cum, Ms, Ep, Zr, Ilm	Gr, Qz'ite, Hf
Nima-otsuka	NO2	Haji	xxx	xx	xx	x	x	xx	Cum, Ms, Zr, Chr, Ilm	Gr, Qz'ite
Nima-otsuka	NO3	Haji	xxx	xx	xx	x	x	x	Zr, Rt, Chr, Ilm,	Gr, Qz'ite
Nima-otsuka	NO4	Sue	xxx	xx	xx	x	–	x	Cum, Zr, Mul, Sp, Ilm	Gr, Qz'ite
Nima-otsuka	NO5	Haji	xxx	xx	xx	x	x	xx	Opx, Ms, Zr, Rt, Ilm, Mgt	Gr, Qz'ite
Nima-otsuka	NO6	Haji	xxx	xx	xx	x	x	xx	Zr, Ilm, Mgt	Gr, Qz'ite
Horen-22	HR	Haji	xxx	xx	xx	x	x	xx	Zr, Ilm	Gr
Oshikiyama	OS	Haji	xxx	xx	xx	x	–	x	Ms, Ep, Zr, Ilm	Gr
Kotsukuriyama	KT	Haji	xxx	xx	xx	x	–	x	Mul, Sp, Ilm	Gr
Kotsukuriyama-nishi-3	KTN	Haji	xxx	xx	xx	x	–	x	Mul, Zr, Ilm	Gr
Iwata-3	IW	Haji	xxx	xx	xx	x	x	x	Opx	Gr
Miyayama-4	MI	Haji	xxx	xx	xx	x	x	x	Cum	Gr
Moriyama	MO1	Sue	xxx	xx	xx	x	–	x	Opx, Mul, Sp	Gr
Moriyama	MO2	Sue	xxx	xx	xx	x	–	x	Opx, Mul, Sp	Gr

Abbreviations: Am, amphibole (hornblende, including altered grains); Apt, apatite; Bt, biotite (altered); Chr, chromite; Cum, cummingtonite; Ep, epidote; Gl, volcanic glass; Gr, granite/granodiorite/aplite/granophyre; Hf, hornfels; Ilm, ilmenite; Kfs, K-feldspar; Mgt, magnetite; Ms, muscovite; Mul, mullite; Opx, orthopyroxene; Pl, plagioclase; Qz, quartz; Qz'ite, quartzite/quartz vein; Rt, rutile; Sp, spinel; Zr, zircon. Modal abundance: xxx > 30 vol%, xx 10–30 vol%, x < 10 vol%, – not detected.

In Sue-type sherds (SZ3, MO1, MO2, and NO4) and two Haji-type sherds (ZZ1 and KTN), some alkali feldspar inclusions have molten rims (Fig. 6f) with an optically isotropic appearance. This is probably an effect of the firing of the *haniwa*, and the compositions of molten rims are excluded from Fig. 8.

4.3.3. Muscovite

Muscovite that occurs in hornfels fragments and granitoid fragments in *haniwa* sherds consistently has similar Fe content and Al/Si ratios to muscovite from nearby outcrops of hornfels and granitoid, respectively (Fig. 9). Most of the discrete grains of muscovite in *haniwa* sherds have similar compositions to those in hornfels outcrops (Fig. 9).

4.3.4. Volcanic glass

The compositions of volcanic glass inclusions in *haniwa* sherds are comparable with those of widespread tephras in southwestern Japan (Albert et al., 2018; Machida and Arai, 1992; Maruyama et al., 2020; Auer et al., 2022), with particular similarities to the Aira-Tanzawa (AT) and Kikai-Akahoya (KA) tephras in SiO_2, TiO_2, and Al_2O_3 content (Fig. 10). However, the content of other elements in *haniwa*, particularly Na_2O, K_2O, and CaO, is variable with no similarities to any tephra (Supplementary Fig. 1a, b). The deviation of the amounts of these components from the typical AT and KA tephras is particularly prominent in Sue-type *haniwa* sherds, suggesting an effect of high-temperature firing.

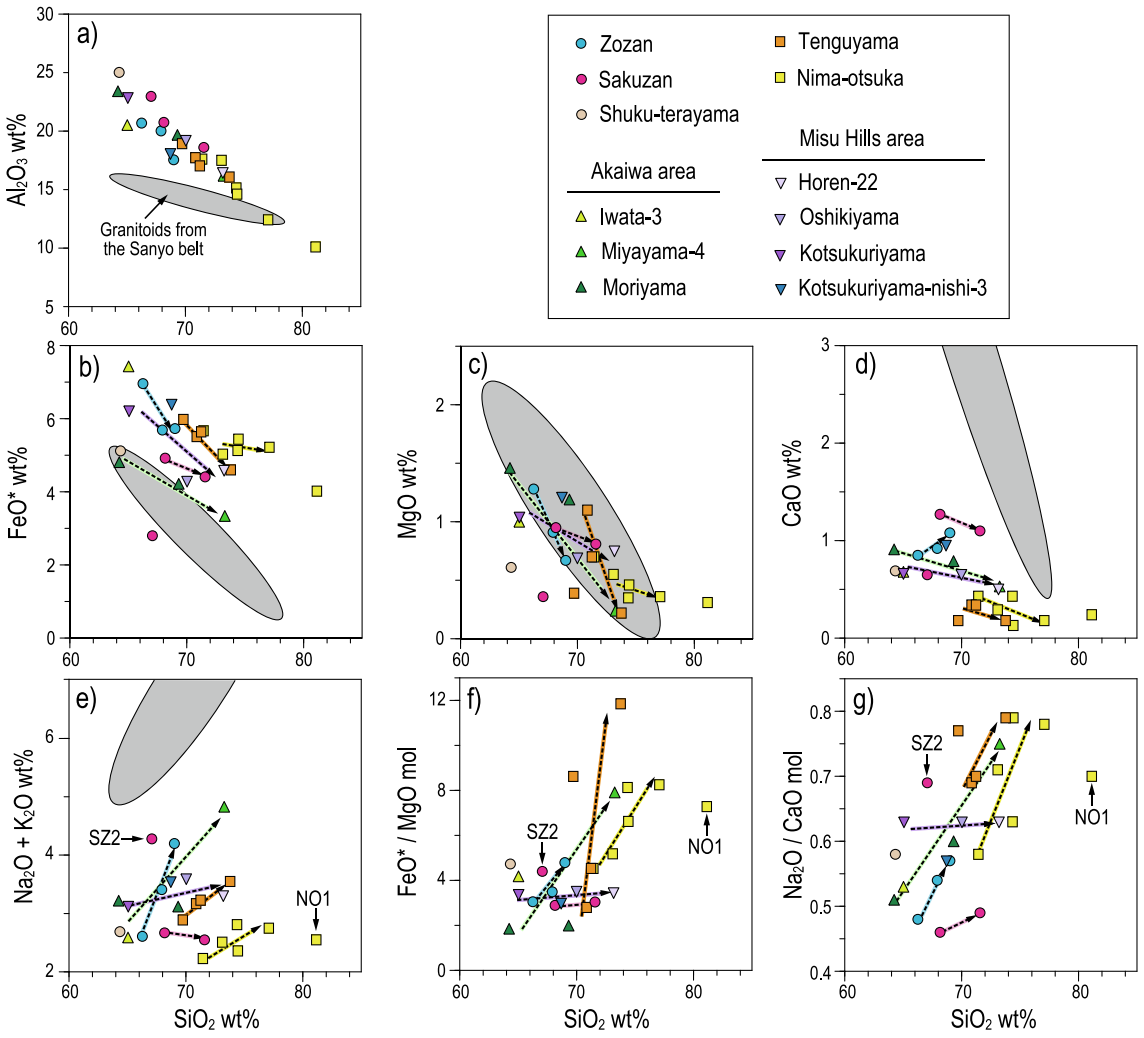

Fig. 5. Variation diagrams of bulk compositions of *haniwa* sherds. Shaded areas represent the compositional ranges of most of granitoids (granites or granodiorites) from the Okayama and Kagawa areas in the Sanyo belt, southwestern Japan (Ishihara, 2003). FeO*: total amount of iron calculated as FeO. Plotted data in (b)-(g) show a systematic increasing/decreasing trend with increasing SiO_2 for each tomb indicated by a dashed line with the same color as the data points, excluding a few noticeably deviating data, e.g., SZ2 and NO1 (see text for discussion).

4.3.5. Matrix

Most of the Haji-type *haniwa* sherds have matrix compositions between kaolinite (or halloysite), pyrophyllite, and di-octahedral smectites including montmorillonite and beidellite, except for the Zozan *haniwa*, which is richer in chlorite or vermiculite component (Fig. 11a-c). The Sue-type *haniwa* sherds from the Sakuzan, Nima-otsuka, and Moriyama mounded tombs show a trend of matrix composition toward alkali feldspar (Fig. 11b), suggesting chemical modification by high-temperature firing.

5. Discussion

The predominance of quartz, K-feldspar, and plagioclase inclusions, the presence of relatively large grains (1–2 mm) and gradual variation of grain size (down to < 10 μm) of these minerals, and the common occurrence of granite or granodiorite fragments (Figs. 3 and 4, Table 2) suggest that the paste materials utilized in *haniwa* production investigated in this study were mainly derived from weathered granitic rocks, including biotite granite and hornblende granodiorite. Although the possibility that different materials were artificially mixed for tempering cannot be ruled out, we have no evidence for this possibility, such as the presence of abundant exotic materials and clear gaps in size, shape, and roundness of inclusions in each sherd (Quinn, 2013). Furthermore, bulk compositional variations can be explained by magmatic differentiation processes rather than mixing of different source materials as discussed below. Even if certain amounts of inclusions were mixed for tempering the clay materials, most of the inclusions in each sherd could be fragments derived from the same granitic body as the source of the clay matrix.

Compared with typical granitic rocks, however, the *haniwa* sherds show a deficiency of Ca, Na, and K and an excess of Al and Fe in bulk compositions (Fig. 5). Considering the much lower abundance of inclusions other than of granitic origin, i.e., tephra, quartz rock, and hornfels, in the *haniwa* sherds, their effects on bulk compositions could be restrictive, except for a few sherd samples with an abundance of these exotic inclusions (e.g., SZ2 and NO1). Instead, the depletion and enrichment of compositions can be explained by chemical weathering of original igneous phases to form clay minerals, for example, by a reaction (Deer et al., 1992):

$$2\ KAlSi_3O_8 + 3\ H_2O \rightarrow Al_2Si_2O_5(OH)_4 + 2\ K(OH)_{(aq)} + 4\ SiO_{2\ (aq)}$$

K-feldspar kaolinite

The depletion of Ca, Na, and K and enrichment of Al and Fe can be ascribed to the decomposition of plagioclase and alkali feldspar to form kaolinite or pyrophyllite and of biotite and amphibole to form smectites,

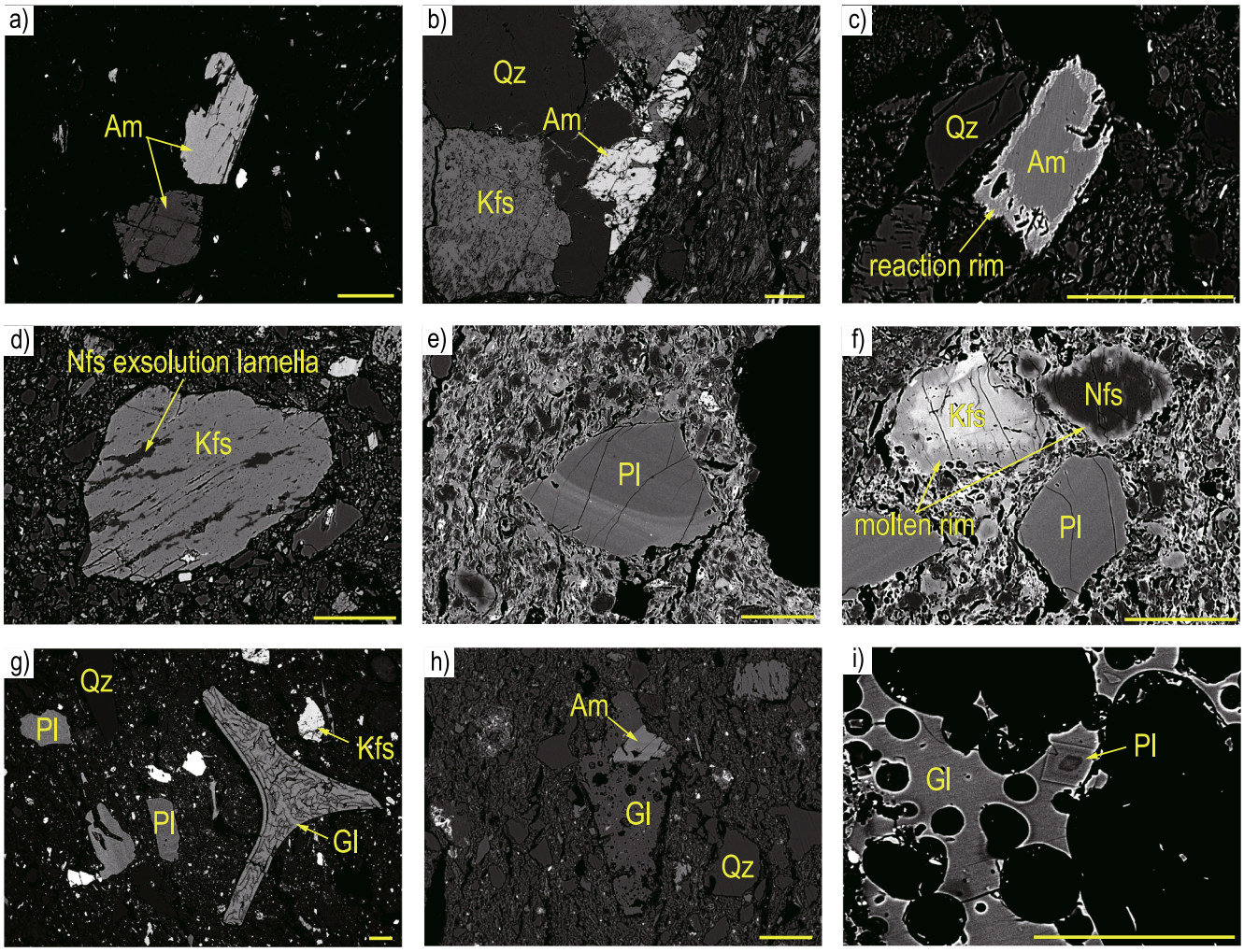

Fig. 6. Back-scattered electron images showing the characteristic modes of occurrence of mineral and rock inclusions. (a) Two types of amphibole grains with different brightness corresponding to Fe/Mg ratio (sample# ZZ2). (b) Granodiorite containing quartz, K-feldspar, and relatively Fe-rich amphibole (ZZ1). (c) Amphibole with a reaction rim (NO6). (d) K-feldspar with exsolution lamellae of Na-feldspar (MI4). (e) Plagioclase with an oscillatory zonal structure (MO2). (f) K-feldspar and Na-feldspar with molten rim (MO2). (g) Bubble-wall-type volcanic glass (NO2). (h) Pumice-type volcanic glass containing relatively Mg-rich amphibole (NO5). (i) Pumice-type volcanic glass containing plagioclase with an oscillatory zonal structure (NO4). Abbreviations for minerals: Am, amphibole; Gl, volcanic glass; Kfs, K-feldspar; Nfs. Na-feldspar; Pl, plagioclase; Qz, quartz. Scale bars indicate 0.1 mm.

chlorite, or vermiculite associated with magnetite or ilmenite formation, which is commonly observed in weathered granitic rocks. The presence of these clay minerals in the *haniwa* paste is indicated by the chemical compositions of the matrix (Fig. 11).

The clay minerals suggested by the matrix chemical compositions, however, were not detected by XRD analyses (Fig. 4). This discrepancy probably represents a firing effect, i.e., dehydration and decomposition of crystal structures during the firing of the *haniwa*. For instance, kaolinite is dehydrated to form disordered meta-kaolinite at ~ 400–800 °C (e.g., Brindley and Nakahira, 1958, 1959), and montmorillonite probably forms amorphous silica and alumina at > 650 °C (Worrall, 1986). At higher temperatures, ~900–1100 °C, the products formed by the heating of kaolinite and montmorillonite convert to mullite and/or spinel (e.g., Grim and Bradley, 1940; Brindley and Nakahira, 1958; Deer et al., 1962), which were detected in Sue-type sherds and some Haji-type sherds by XRD analyses in this study (Fig. 4, Table 2). Decomposition of the clay crystal structure to form amorphous phases and/or melting during firing is also suggested by the low optical activity of the matrix (Quinn, 2013) and chemical modification toward alkali feldspar composition in Sue-type sherds (Fig. 11). Additional evidence for a firing effect is the existence of molten rims of feldspar in Sue-type sherds and some of the Haji-type sherds (Fig. 6f). Furthermore, the amphibole reaction rim with low alkali content (Fig. 6c and 7d) and the disappearance of amphibole peaks in XRD patterns (Fig. 4) in Sue-type and some Haji-type sherds could be the results of high-temperature firing as well. The temperature conditions of firing will be reported and discussed elsewhere.

In spite of the chemical modification by weathering and firing, the bulk compositions of *haniwa* sherds seem to retain the relative abundance of the chemical components of original granitic rocks. The bulk contents of Al, Fe, Mg, and Ca decrease with increasing Si (Fig. 5). These compositional variations can be explained by the magmatic differentiation in granitic systems. Supporting evidence for this explanation is provided by the systematic increases of FeO*/MgO and Na_2O/CaO ratios with increasing SiO_2 (Fig. 5f and 5g), which are possible trends resulting from the crystallization of mafic mineral and plagioclase solid solutions that continuously react with evolving magma. Each mounded tomb appears to have an inherent differentiation trend indicated by the arrays of data points on the variation diagrams (Fig. 5b-g). However, there are a few exceptional samples that show noticeable deviation from the trends, probably due to a large amount of mixing with components other than granitic rocks. For example, one sample from Nima-otsuka (NO1) containing large quartz rock fragments has significantly higher SiO_2 content (> 80 wt%) and one sample from Sakuzan (SZ2) with a higher

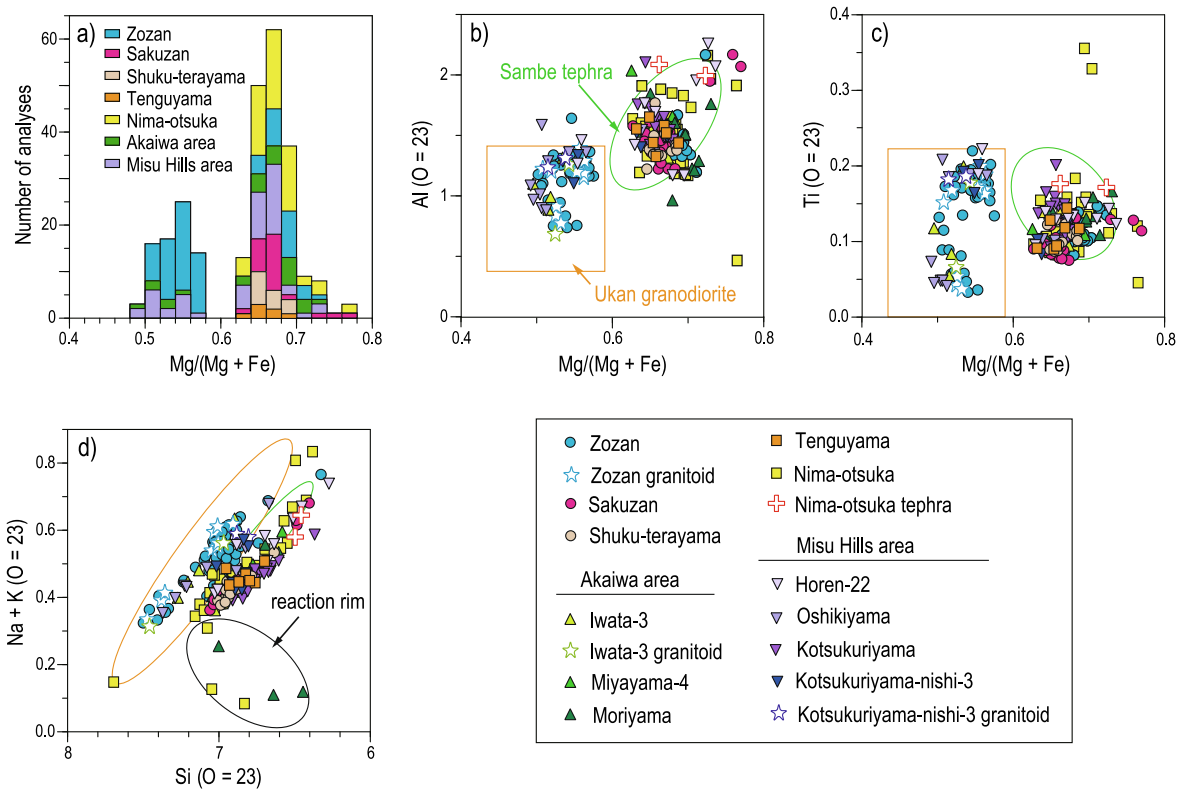

Fig. 7. Chemical compositions of calcic amphibole. (a) Frequency diagram of Mg/(Mg + Fe) mol ratio. (b-d) Plots of Al and Ti versus Mg/(Mg + Fe), and Na + K versus Si (atoms per formula unit calculated on the basis of 23 oxygen atoms). Plotted data are from discrete grains in the matrix, and component grains of granitoid and tephra (volcanic glass) fragments in *haniwa* sherds from each tomb. Compositions of reaction rims with alkali depletion are encircled in (d). Also shown are typical compositional ranges of amphibole in granodiorites from the Ukan area (Takagi, 1992), and those in tephras from the Sambe volcano (Hattori et al., 1983).

content of Na_2O + K_2O contains muscovite and biotite, which are lacking in the other samples (SZ1 and SZ3). Apart from these exceptional samples affected by exotic inclusions, the inherent magmatic differentiation trends suggest that paste materials used for *haniwa* were collected from a site or neighboring sites in the proximity of granitic bodies, which have local variations in composition between the sites of material collection for each mounded tomb. Significant variations in bulk chemical compositions of *haniwa* from Sakuzan and Zozan have been reported and ascribed to the difference in mining site of paste materials (Harunari et al., 2016). The possibility of the existence of different mining sites for each mounded tomb cannot be ruled out, and analyses of additional *haniwa* samples will be required to address this issue.

Compared with the major granitic components, inclusions of tephra origin are less voluminous but commonly included in all the samples, and are therefore significant for characterization of *haniwa* produced in the Kibi region. Inclusions of volcanic glass have compositions, particularly Ti and Al contents, that are relatively immobile during alteration in natural rocks, suggestive of their Aira-Tanzawa (AT) and Kikai-Akahoya (KA) tephra origin (Fig. 10). These widespread tephras are dominated by bubble-walled glass (Machida and Arai, 1992, 2003), in agreement with the morphology of glass inclusions observed in the *haniwa* sherds (Figs. 3 and 6g).

The compositional variations of amphibole and plagioclase also suggest the mixing of tephra and granitic components. The Fe-richer and Mg-richer groups of amphibole seem to be derived from granodiorite and tephra, respectively (Fig. 6a, 6b, 6h, and 7a-d). The modes of occurrence (Fig. 6e and 6i) and chemical compositions (Fig. 8) of feldspar suggest that relatively An-rich plagioclase could be derived from tephra, whereas Ab-rich plagioclase and K-feldspar derive from granitic rocks (Fig. 6b, 6d, and 8). However, the AT and KA tephras, from which volcanic glass in the *haniwa* sherds is possibly derived, are not associated with amphibole (Machida and Arai, 1992). A possible source of amphibole-bearing tephra in the Chugoku region of southwestern Japan is the Sambe or Daisen volcano (Tsukui, 1984; Hayashi and Miura, 1987; Machida and Arai, 1992). Of these, the most probable source of amphibole and plagioclase in the *haniwa* sherds is the Sambe-Ukinuno (SU) or Sambe-Ikeda (SI) pumice fall, which contains much more abundant amphibole and plagioclase than other minerals and is widely distributed in the Kibi region (Fig. 1; Hayashi and Miura, 1987; Machida and Arai, 1992; Maruyama et al., 2020). Consistently, volcanic glass inclusions associated with amphibole and plagioclase in the *haniwa* sherds have a morphology of pumice type (Fig. 6h and 6i), which is different in shape and compositions from the bubble-wall type that is commonly included in the *haniwa* sherds and the AT and KA tephras (Fig. 6g and 10). The composition of plagioclase-associated glass in the Nima-otsuka *haniwa* is similar to typical SU and SI glass (Albert et al., 2018; Auer et al., 2022; Maruyama et al., 2020a), but that of amphibole-associated glass looks different (Fig. 10). However, some silica-rich glass fragments in SU tephra were also reported (Maruyama et al., 2020b), which have compositions similar to the amphibole-associated glass in the *haniwa* sherd. Further evidence for the Sambe tephra origin of amphibole in *haniwa* is provided from the similarity in the chemical compositions of amphibole (Fig. 7; Hattori et al., 1983).

The above descriptions and discussions can be summarized as follows. The materials of *haniwa* examined in this study are commonly derived from weathered granitic rocks with the addition of small amounts of tephra components originating from the Aira, Kikai, and Sambe volcanos. Variations in the abundance of mineral/rock inclusions, bulk compositions, and mineral compositions reflect the characteristics of local geologic settings. For example, differences in the bulk chemical composition trend between mounded tombs (Fig. 5) could be a reflection of the compositions of granitic rocks with variable magmatic differentiation. Relatively FeO- and MgO-rich bulk

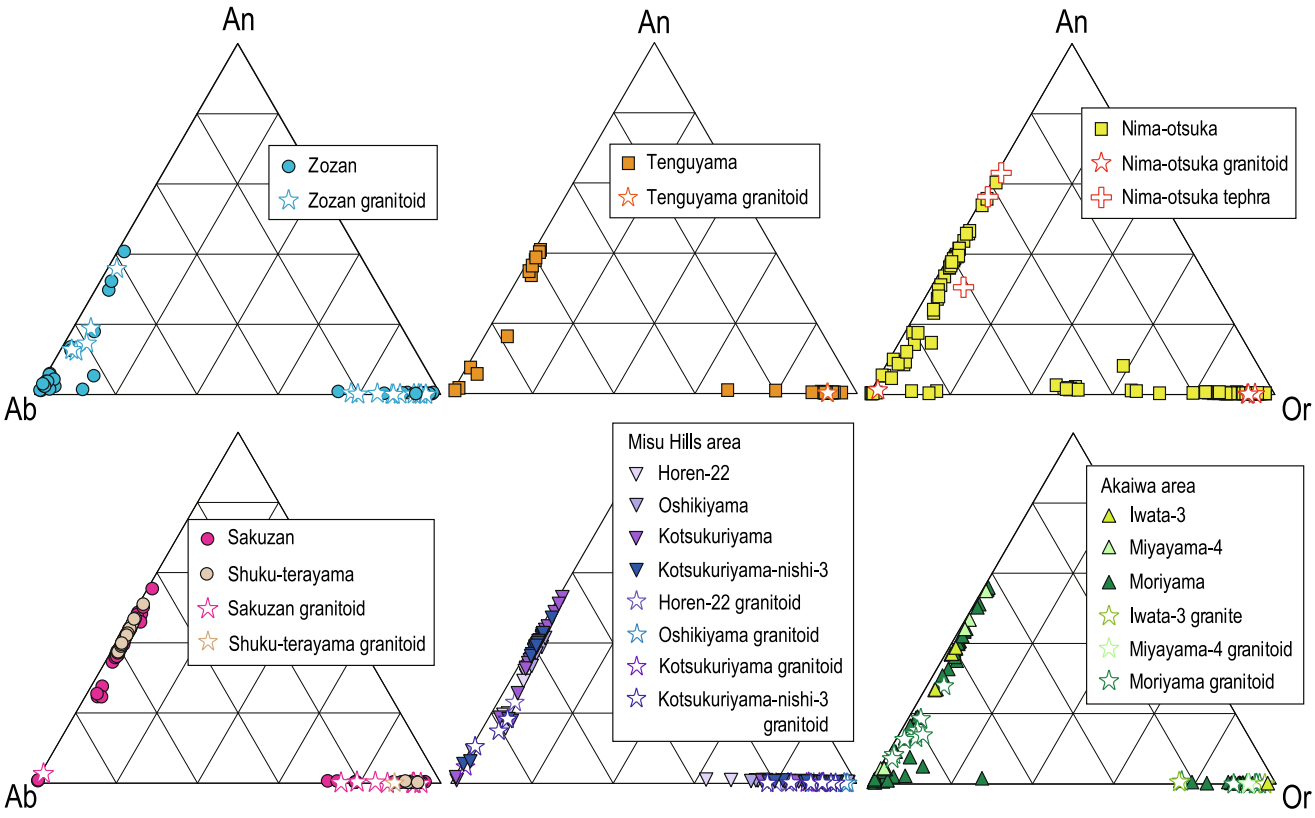

Fig. 8. Ternary An-Ab-Or (anorthite, $CaAl_2Si_2O_8$; albite, $NaAlSi_3O_8$; orthoclase, $KAlSi_3O_8$; mol ratio) diagrams of feldspar. Plotted data are from discrete grains in the matrix and component grains of granitoid and tephra (volcanic glass) fragments in *haniwa* sherds from each tomb, including cores and rims of zoned plagioclase and exsolution lamellae of alkali feldspar, and excluding molten rims.

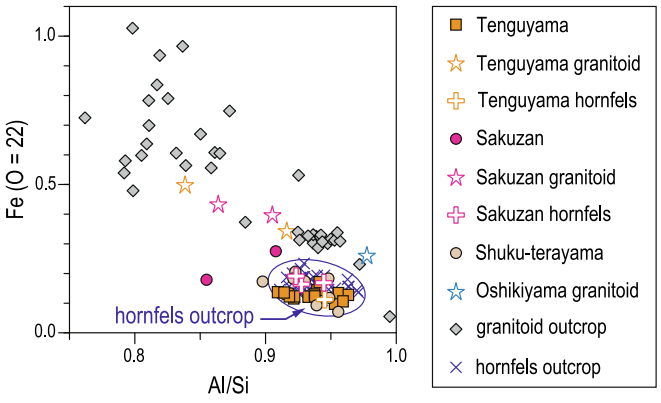

Fig. 9. Fe (atoms per formula unit calculated on the basis of 22 oxygen atoms) versus Al/Si mol ratio of muscovite. Plotted data are from discrete grains in the matrix and component grains of granitoid and hornfels fragments in *haniwa* sherds. Also plotted are compositions of muscovite in granitoid and hornfels samples from outcrops near the Nima-otsuka and Tenguyama mounded tombs. The data from hornfels is encircled.

compositions (Fig. 5), the occurrence of Fe-richer amphibole (Fig. 7), and the dominance of chlorite/vermiculite in the matrix (Fig. 11) of *haniwa* from Zozan could be caused by wide exposure of granodiorite in an upriver area of the Ashimori River (Fig. 1). The abundance of muscovite, hornfels, and quartz rock inclusions (Table 2) and resulting deviation from common trends of bulk chemical compositions (Fig. 5) in some *haniwa* sherds from Sakuzan and Nima-otsuka could be caused by nearby exposures of hornfels of mudstone origin (Fig. 1). In addition, it is noteworthy that Nima-otsuka *haniwa* sherds contain, though sparsely, small grains of chromite, which never occurs in granitic rocks and other rocks exposed in the surrounding area nor widespread tephras in southwestern Japan, but occurs almost restrictedly in ultramafic rocks in this region. The most likely source of the chromite grains is ultramafic rocks (mainly serpentinized peridotites) exposed tens of kilometers northwest of the Nima-otsuka mounded tomb (Fig. 1). Weathered ultramafic rocks including chromite could be transported by the Takahashi River system to the mining site of the *haniwa* paste materials.

In the Kofun period, after the Holocene transgression in Japan, the coastline of the Seto Inland Sea was close to the mounded tomb sites of the Kibi region and a narrow alluvial plain was restricted to the northern areas of the modern plain (Fig. 1; e.g., Archaeological Research Center, Okayama University, 2016). If the paste materials for the *haniwa* were mined from the alluvial plain of the Kofun period, the mineral and rock inclusions in the *haniwa* should be highly variable as usually observed in deposits transported by big river systems. This study, however, has revealed that the majority of the *haniwa* of the Kibi region is uniformly composed of two or three components, i.e., dominant weathered granitic rocks and subordinate tephras. The three widespread tephras included in the *haniwa*, AT, SU, and KA (Fig. 1), erupted ~ 30000, ~20000, and ~ 7300 years ago, respectively (Smith et al., 2013; Albert et al., 2018, 2019; Maruyama et al., 2020b), and probably remained on land in the Kofun period as relatively thick layers covering the basement of weathered granitic rocks. It follows that the mixing of the widespread tephra with granitic materials did not need transportation by a big river system.

Considering the abundance of clay minerals, highly variable grain size of inclusions, and the bulk compositions reflecting the local variation of the degree of magmatic differentiation, it is likely that the paste materials of the *haniwa* originated from weathered granitic rocks that were exposed around each mounded tomb and subsequently eroded and transported a short distance, involving nearby hornfels and quartz rock in some cases, and then deposited at mining sites, retaining the original

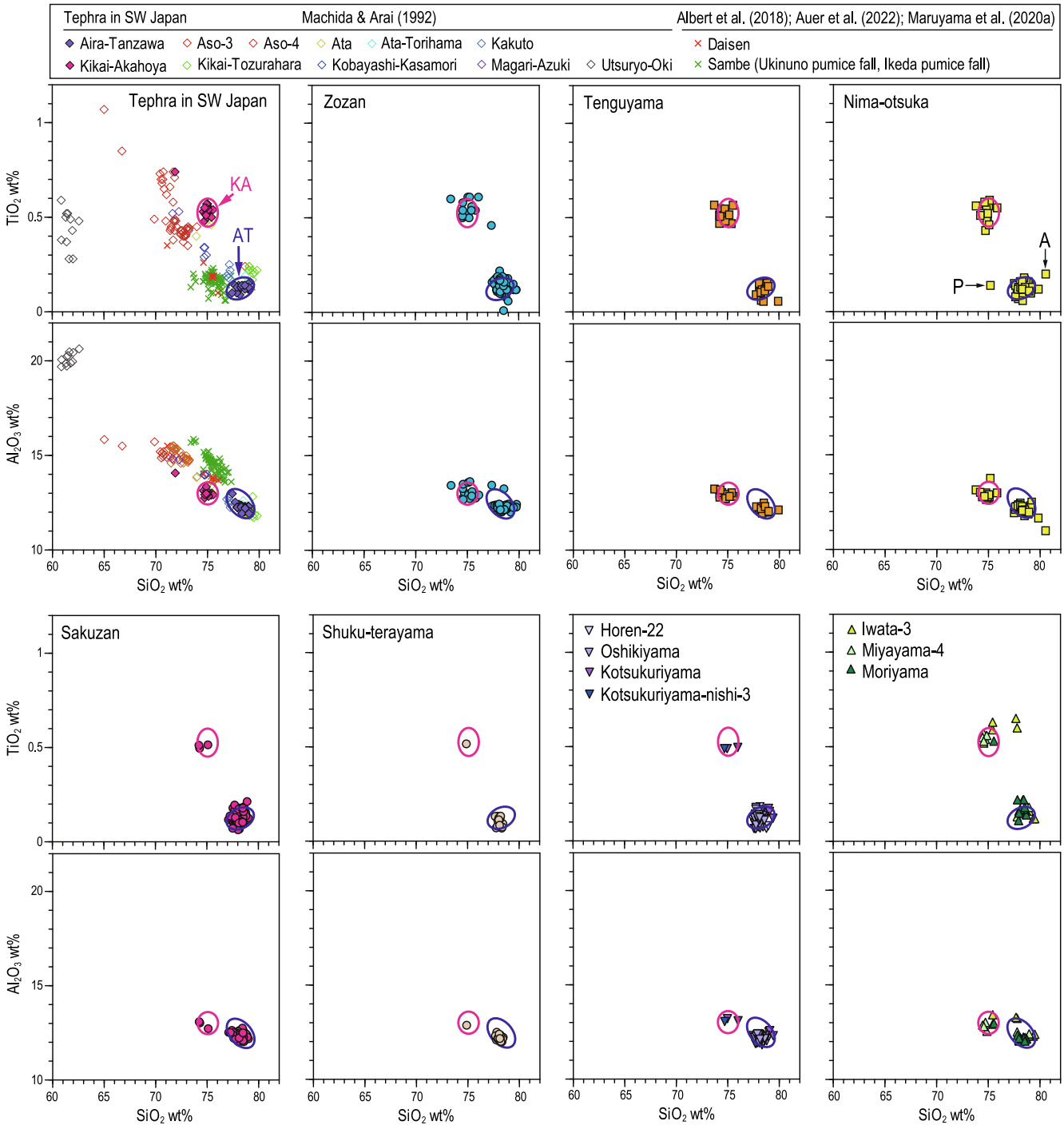

Fig. 10. TiO_2 versus SiO_2 and Al_2O_3 versus SiO_2 diagrams (volatiles-free base) for volcanic glass in *haniwa* sherds and Quaternary widespread tephras in south-western Japan compiled from the literature (Machida and Arai, 1992; Albert et al., 2018; Auer et al., 2022; Maruyama et al., 2020a). The data of Sambe tephra are from proximal deposits of the Sambe-Ukinuno pumice fall and Sambe-Ikeda pumice fall units, which possibly fell in the Kibi region. Encircled areas represent typical compositions of Aira-Tanzawa (AT) and Kikai-Akahoya (KA) tephras, which are similar to the compositions of volcanic glass in *haniwa* sherds. Plots with letters "A" and "P" in the TiO_2 versus SiO_2 diagram of Nima-otsuka indicate amphibole-bearing and plagioclase-bearing glass, respectively.

compositional characteristics. The mining sites of paste materials were probably located at the bases of hills of granitic rocks covered by widespread tephras and in some cases, near the flood plain of river systems transporting some materials such as chromite from a distance.

The multi-technique petrological analyses adopted in this study successfully revealed similarities and differences in the mineralogical and chemical compositions of *haniwa* among mounded tombs in the Kibi region. Similar analyses of *haniwa* from other regions and comparative studies are expected to advance our understanding of the uniqueness of the material provenance of *haniwa* from each region, the interaction between regions, and the cultural and technological development of ancient Japanese society.

6. Conclusions

The results of multi-technique petrological analyses indicate that the

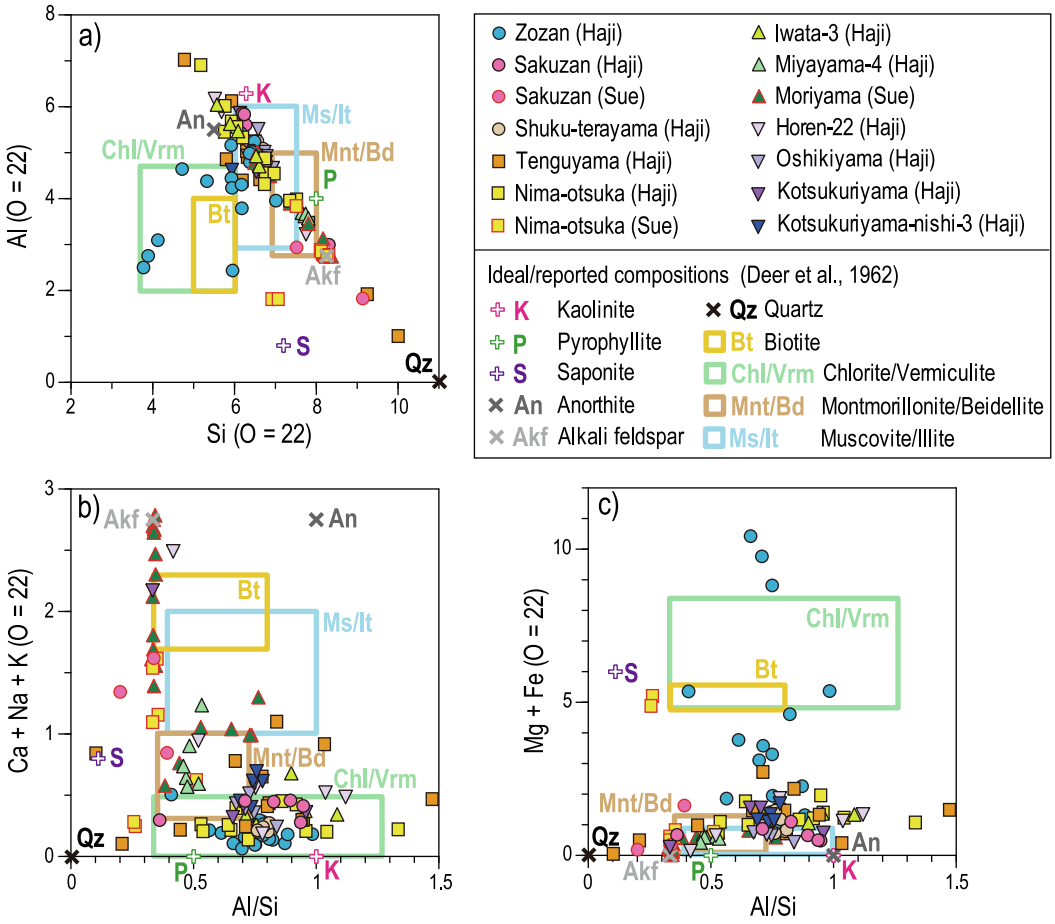

Fig. 11. Compositions of the clay matrix of *haniwa* sherds. (a) Al versus Si (atoms per formula unit calculated on the basis of 22 oxygen atoms). (b) Ca + Na + K versus Al/Si mol ratio. (c) Mg + Fe versus Al/Si mol ratio. Compositional ranges of ideal or reported clay and related minerals (after Deer et al., 1962) are shown for comparison.

paste materials of studied *haniwa* were commonly derived from weathered granitic rocks mixed with minor amounts of three widespread tephras erupted from the Aira, Kikai and Sambe volcanos, which could be one of the significant characteristics of *haniwa* produced in the Kibi region. In addition, the *haniwa* sherds show variations in chemical and mineralogical compositions between tombs, which are probably affected by local geologic settings, suggesting the presence of specific mining sites of paste materials around each tomb. The mining sites could be located at the bases of hills of granitic rocks covered by widespread tephras and in some cases, near the flood plain of big river systems.

CRediT authorship contribution statement

Toshio Nozaka: Writing – original draft, Visualization, Supervision, Methodology, Investigation, Conceptualization. **Naoya Ohbayashi:** Visualization, Investigation. **Yuki Toda:** Visualization, Investigation. **Kanako Sugiura:** Investigation. **Takahiro Nozaki:** Writing – review & editing, Resources, Investigation, Conceptualization. **Osamu Kimura:** Writing – review & editing, Resources, Investigation, Conceptualization. **Naoko Matsumoto:** Writing – review & editing, Resources, Conceptualization. **Akira Seike:** Writing – review & editing, Supervision, Resources, Funding acquisition, Conceptualization.

Acknowledgments

The *haniwa* sherd samples used in this study were provided by Akaiwa City, Kurashiki City, Okayama City, Soja City, and Okayama University. We are grateful to Y. Benino, T. Nanba and Y. Nishina for permission to use the XRF and XRD equipment in their laboratory at Okayama University and to C. Nakano for supporting our XRD analyses. Our special thanks go to J. Ryan for reading the manuscript and providing valuable suggestions. The manuscript was improved by comments from two anonymous reviewers. This study was financially supported by JSPS KAKENHI Grant Number 20H05634.

Appendix A. Supplementary data

Supplementary data to this article can be found online at https://doi.org/10.1016/j.jasrep.2024.104813.

Data availability

Data are contained in the manuscript as a supplementary file.

References

Albert, P.G., Smith, V.C., Suzuki, T., McLean, D., Tomlinson, E.L., Miyabuchi, Y., Kitaba, I., Mark, D.F., Moriwaki, H., SG06 Project Members, Nakagawa, T., 2019. Geochemical characterisation of the Late Quaternary widespread Japanese tephrostratigraphic markers and correlations to the Lake Suigetsu sedimentary archive (SG06 core). Quaternary Geochronology, 52, 103-131.

Albert, P.G., Smith, V.C., Suzuki, T., Tomlinson, E.L., Nakagawa, T., McLean, D., Yamada, M., Staff, R.A., Schlolaut, G., Takemura, K., Nagahashi, Y., Kimura, J., Suigetsu 2006 Project Members, 2018. Constraints on the frequency and dispersal of explosive eruptions at Sambe and Daisen volcanoes (South-West Japan Arc) from the distal Lake Suigetsu record (SG06 core). Earth Sci. Rev. 185, 1004–1028.

Archaeological Research Center, Okayama University, 2016. The Yayoi period in the Kibi region. Kibito Publishing Inc., Okayama, 136p. (in Japanese, title translated).

Auer, A., Kamei, A., Endo, D., 2022. Sanbe volcano: Long-term evolution of an arc magmatic system. Isl. Arc 31, e12453.
Bence, A.E., Albee, A.L., 1968. Empirical correction factors for the electron microanalysis of silicates and oxides. J. Geol. 76, 382–403.
Brindley, G.W., Nakahira, M., 1958. A new concept of the transformation sequence of kaolinite to mullite. Nature 181, 1333–1334.
Brindley, G.W., Nakahira, M., 1959. The kaolinite-mullite reaction series: II, metakaolin. J. Am. Ceram. Soc. 42, 314–318.
Cox, K.G., Bell, J.D., Pankhurst, R.J., 1979. The Interpretation of Igneous Rocks. George Allen & Unwin, London, 450p.
Deer, W.A., Howie, R.A, Zussman, J., 1962. Rock- Forming Minerals, vol. 3, Sheet Silicates. Longman, London, 270p.
Deer, W.A., Howie, R.A, Zussman, J., 1992. An Introduction to the Rock-forming Minerals, 2nd Edition. Longman, Essex, 696p.
Geological Survey of Japan, 2022. Seamless digital geological map of Japan v.2 1: 200,000. https://gbank.gsj.jp/seamless (accessed 12 Sep. 12, 2022).
Grim, R.E., Bradley, W.F., 1940. Investigation of the effect of heat on the clay minerals illite and montmorillonite. J. Am. Ceram. Soc. 23, 242–248.
Harunari, H., Nakazono, S., Hirakawa, H., Tarora, M., Wakamatsu, K., 2016. Provenance investigation of *haniwa* from Zozan, Sakuzan, and Shuku-terayama mounded tombs in Okayama Prefecture. Okayama City Archaeol. Center Rep. 8, 49–81 (in Japanese, title translated).
Hattori, H., Kano, K., Suzuki, T., Yokoyama, S., Matsuura, H., Satoh, H., 1983. Quadrangle Series 1: 50,000 Geology of the Sambesan District. Geol. Surv. Japan, Tsukuba, 175p (in Japanese with English abstract).
Hayashi, M., Miura, K., 1987. Stratigraphy and distribution of tephra arising from Sambe volcano. Stud. the San'in Region: Nat. Environ. 3, 43–66 (in Japanese with English abstract).
Heiken, G., 1972. Morphology and petrography of volcanic ashes. Geol. Soc. Am. Bull. 83, 1961–1988.
Hirakawa, H., Nakazono, S., Tarora, M., Wakamatsu, K., Harunari, H., 2018. X-ray fluorescence analysis of *haniwa* from Tsukuriyama (Zozan), Tsukuriyama (Sakuzan), and the surrounding kofun tumulus in Okayama Prefecture, Japan. Pap. Proc. Jpn. Assoc. Archaeoinformatics 21, 76–81 (in Japanese).
Ishihara, S., 2003. Chemical contrast of the Late Cretaceous granitoids of the Sanyo and Ryoke Belts, Southwest Japan: Okayama-Kagawa Transect. Bull. Geol. Surv. Jpn. 54, 95–116.
Kimura, O., 2023. Chronology of cylindrical *haniwa* in the first half of the Middle Kofun period in the Kibi region. Kodai Kibi, 34, 31-50 (in Japanese, title translated).
Kondo, Y., Harunari, H., 1967. The origin of *haniwa*. Quart Archaeol. Stud. 13, 13–35 (in Japanese, title translated).
Le Bas, M.J., Le Maitre, R.W., Streckeisen, A., Zanettin, B., 1986. A chemical classification of volcanic rocks based on the total alkali-silica diagram. J. Petrol. 27, 745–750.
Machida, H., Arai, F., 1992. Atlas of Tephra in Japan and its Surrounding Area. University of Tokyo Press, Tokyo, 276p (in Japanese, title translated).
Machida, H., Arai, F., 2003. Atlas of Tephra in Japan and its Surrounding Area, 2nd Edition. University of Tokyo Press, Tokyo, 336p (in Japanese, title translated).
Maruyama, S., Takemura, K., Hirata, T., Yamashita, T., Danhara, T., 2020a. Major and trace element abundances in volcanic glass shards in visible tephras in SG93 and SG06 drillcore samples from Lake Suigetsu, central Japan, obtained using femtosecond LA–ICP–MS. J. Quat. Sci. 35, 66–80.
Maruyama, S., Yamashita, T., Hayashida, A., Hirata, T., Danhara, T., 2020b. Examination of the relationship between the Ukinuno and Sakate tephras from Sambe volcano, Southwest Japan. J. Geogr. 129, 375–396.
Nakamura, Y., Kushiro, I., 1970. Compositional relations of coexisting orthopyroxene, pigeonite and augite in a tholeiitic andesite from Hakone volcano. Contrib. Miner. Petrol. 26, 265–275.
Nozaki, T., 2017. Construction of a widespread chronology of *haniwa* of the Middle Kofun period in the Chugoku region, in: Executive Committee of Research Society of Keyhole-Shaped Mounded Tombs in the Chugoku and Shikoku Regions (Ed.), Current Status and Issues of Research about Mounded Tombs in the Middle Kofun Period: Difference between the Widespread Chronology and Regional Chronologies, pp. 21-30 (in Japanese, title translated).
Okuda, H., 1990. Stone material and *haniwa* of the Zozan mounded tomb. Studies in archeology: Proceedings of the Archaeological Institute of Kashihara, 14, 65-94 (in Japanese, title translated).
Quinn P.S., 2013. Ceramic Petrography: The Interpretation of Archaeological Pottery & Related Artefacts in Thin Section. Archaeopress, Oxford. 251p.
Smith, V.C., Staff, R.A., Blockley, S.P.E., Ramsey, C.B., Nakagawa, T., Mark, D.F., Takemura, K., Danhara, T., Suigetsu 2006 Project Members, 2013. Identification and correlation of visible tephras in the Lake Suigetsu SG06 sedimentary archive, Japan: chronostratigraphic markers for synchronising of east Asian/west Pacific palaeoclimatic records across the last 150 ka. Quaternary Science Reviews, 67, 121-137.
Takagi, T., 1992. Mineral equilibria and crystallization conditions of Ukan granodiorite (ilmenite-series) and Kayo granite (magnetite-series), San'yo Belt, Southwest Japan. J. Geol. Soc. Jpn 98, 101–124.
Tsukui, M., 1984. Geology of Daisen volcano. J. Geol. Soc. Jpn 90, 643–658 (in Japanese with English abstract).
Wilson, M., 1989. Igneous Petrogenesis. Springer, Dordrecht, 466p.
Worrall, W.E., 1986. Clays and Ceramic Raw Materials, 2nd Edition. Elsevier Applied Science Publishers, Essex, 239p.